THE CRYSTAL STRUCTURE OF TALNAKHITE, $Cu_{18}Fe_{16}S_{32}$.[1]

S. R. HALL AND E. J. GABE,[2] *Department of Energy, Mines and Resources, Mines Branch, Ottawa, Canada K1A 0G1*

ABSTRACT

Talnakhite is a Cu–Fe sulphide first reported by Bud'ko and Kulagov (1963) as having a composition of $CuFeS_{1.8}$ and a cubic unit cell with $a = 5.28$ Å. They proposed that this was the natural equivalent of synthetic high-temperature chalcopyrite ($a = 5.26$ Å). Subsequent work by Genkin *et al.* (1966) and Cabri (1967) suggested that talnakhite has a larger cubic unit cell with $a = 10.6$ Å, similar to that of synthetic β–phase (Hiller and Probsthain, 1956). This study shows talnakhite to have a cell with $a = 10.593$ Å, space group $I\bar{4}3m$ and a partially–ordered structure which is consistent with both the β–phase and the metal-rich stoichiometric composition of $Cu_{18}Fe_{16}S_{32}$ (Cabri and Harris, 1971).

INTRODUCTION

Talnakhite is a Cu–Fe sulphide occurring, in concentrations of up to 70 percent, in the vein ores of the Noril'sk and Talnakh deposits, Western Siberia, U.S.S.R. The new mineral was first discovered by Bud'ko and Kulagov (1963) following difficulties with the extraction of chalcopyrite by the flotation process. They reported that talnakhite was distinguishable from chalcopyrite ($CuFeS_2$) by its different optical properties and X–ray powder data, and the sulphur–deficient composition $CuFeS_{1.8}$. Bud'ko and Kulagov described the crystal cell as cubic with $a = 5.28$Å and considered it the natural equivalent to the synthetic high–temperature form of chalcopyrite with $a = 5.26$Å (Donnay and Kullerud, 1958). This conclusion was of mineralogical importance as high–temperature chalcopyrite is generally considered unstable at room temperature unless rapidly quenched from above 550°C (Yund and Kullerud, 1966). Although the presence of zinc was postulated as a possible reason for the unusual stability of "small–cell" talnakhite, the occurrence of such a large deposit at Noril'sk implied a rather extraordinary geological history.

These conclusions prompted further investigation into the nature of talnakhite. Genkin *et al.* (1966) reported that the X–ray diffraction powder pattern of talnakhite was also consistent with the synthetic β–phase ($Cu_{17+x}Fe_{17+x}S_{32}$, $x \simeq 0.6$) of Hiller and Probsthain (1956) and appeared to form an intergrowth with chalcopyrite in the ore body.

They concluded therefore that talnakhite was a partially ordered phase intermediate between the normal ordered chalcopyrite (Pauling and Brockway, 1932) and a disordered small cubic cell phase unstable at room temperature. The electron microprobe analyses of Genkin *et al.* (1966) and Cabri (1967) failed to detect the presence of zinc in the new mineral. The authors pointed out that the presence of sphalerite would account for the zinc reported in the original analysis.

Cabri (1967) found that the Noril'sk ore sample contained two minerals with the (Cu,Fe) : S ratio close to unity. When physically separated, one of these was chalcopyrite itself and the other gave a more extensive diffraction pattern, particularly in the low–angle region, than the data of either Bud'ko and Kulagov (1963) or Genkin *et al.* (1966). All the lines on this pattern could be indexed assuming the body-centred cell of β-phase except for two weak reflections due to a small chalcopyrite impurity. Cabri therefore proposed that the mineral talnakhite was in fact the natural form of the β–phase rather than of high–temperature chalcopyrite. Electron microprobe analyses first suggested that the stoichiometry for this mineral was $Cu_{18}Fe_{18}S_{32}$ similar to that stated for the β–phase. Subsequent analyses on a larger number of natural and synthetic samples indicate, however, that the composition is closer to the stoichiometry $Cu_{18}Fe_{16}S_{32}$ (Cabri and Harris, 1971). The formula may also be written as $Cu_9Fe_8S_{16}$.

EXPERIMENTAL

The crystals of talnakhite were obtained from Dr. L. J. Cabri of the Mineral Sciences Division. These occur as irregular fragments which show no observable twinning effects but have a relatively high mosaic spread. Attempts to grind these fragments to spheres were unsuccessful and a crystal approximating a parallelepiped was selected for further work. The dimensions were approximately $0.1 \times 0.2 \times 0.2$ mm.

Precession films of the 0*kl*, 1*kl*, 2*kl*, *h*0*l*, *h*1*l*, *h*2*l*, and *h*3*l* levels show only reflections satisfying the condition $h + k + l = 2n$ and Laue symmetry $m3m$. This permits three possible space groups; $I432$, $I\bar{4}3m$, and $Im3m$. The films also show a marked superlattice pattern, in which reflections with $h, k, l = 2n$ and $h + k, h + l = 4n$ are the most intense and this suggests the presence of a sphalerite–like subcell with $a = 5.3$ Å. The tetrahedral coordination in such a subcell is not permitted for the spacegroups $I432$ and $Im3m$. The spacegroup $I\bar{4}3m$ was therefore selected as the correct one on the basis of the superlattice reflections.

The final cell parameters were derived using a least squares method applied to the diffractometer angles 2θ, ϕ, χ, and ω, and assuming a triclinic cell. These angles were obtained from an automatic alignment process (Busing, 1970) on the 24 equivalents of the 0, 4, 12 reflection. This gave the values $a = b = c = 10.593(3)$ Å and $\alpha = \beta = \gamma = 90.00(3)°$. The cell contents were established by electron probe analysis (Cabri and Harris, 1971) as:

$$Cu = 27.10 \ (13) \ \text{atomic percent}$$
$$Fe = 24.15 \ (15) \ \text{atomic percent}$$
$$Ni = \ 0.59 \ (05) \ \text{atomic percent}$$
$$S \ = 48.16 \ (13) \ \text{atomic percent}$$

giving a chemical formula of $Cu_{17.9}(Fe_{15.9}Ni_{0.4})S_{31.8}$ and the stoichiometry Cu_{18} $Fe_{16}S_{32}$. The calculated density of 4.28 g cm^{-3}, assuming one formula per unit cell, compares favourably with the value 4.24(5) g cm^{-3} measured pycnometrically (Cabri, 1967). With this formula and density, the linear absorption coefficient $\mu = 142.8$ cm^{-1} for MoKα radiation.

The initial intensity data of talnakhite were collected some two years ago and have been recollected on a number of occasions since as the data collection facilities improved. The nature of the superlattice means that the intensities of about 75 percent of the reflections are relatively weak, and this necessitated more than usual care with the counting statistics. In the initial measurement of intensities only about 12 percent of the reflections were considered significant at the 10 percent statistical level [i.e., $I(\text{net}) > 1.65\sigma(I)$]. Subsequent measurements increased the proportion of observable reflections until finally 189 of the 528 examined in the 2θ range from 0° to 90° (MoKα radiation) were accepted using the above criterion, and subsequently considered 'observed'.

The final measurements were made on an automatic 4-circle diffractometer[1] using graphite monochromatized MoKα radiation. The $\theta/2\theta$ scan width (3–3.5°) was adjusted for dispersion. Background counts were measured each side of the peak, for approximately the same length of time as that taken for the scan. The intensities of three reference reflections were recorded after every 25 measurements in order to monitor the crystal alignment and instrumental stability. No significant variation in the intensities of the reference reflections was observed during the data collection process.

Absorption corrections were computed (Gabe and O'Byrne, 1970) by Gaussian integration for the crystal shape and μ-value described above and applied to the net intensities averaged from three separate measurements. The normal Lorentz and polarization factors were applied to produce a set of observed structure factors from these values.

STRUCTURE DETERMINATION

Although there were significant differences in composition between the synthetic β–phase (Hiller and Probsthain, 1956) and talnakhite, it was anticipated from diffraction data that their structures would be very similar. However, because the model for the β-phase was proposed from limited data and not refined, the present determination was carried out independently.

The distribution of diffraction intensities indicated that talnakhite, to a first approximation, could be considered initially in terms of a disordered sphalerite–like (Cu, Fe)S cell, which was related to the 10.6Å cell by the diagonal transformation matrix [1/2, 1/2, 1/2] and the

- ● METAL 1 (0,0,0)
- ◯ METAL 2 (X,0,0)
- ◎ METAL 3 (1/2,1/4,0)
- ○ METAL 4 (X,X,X)
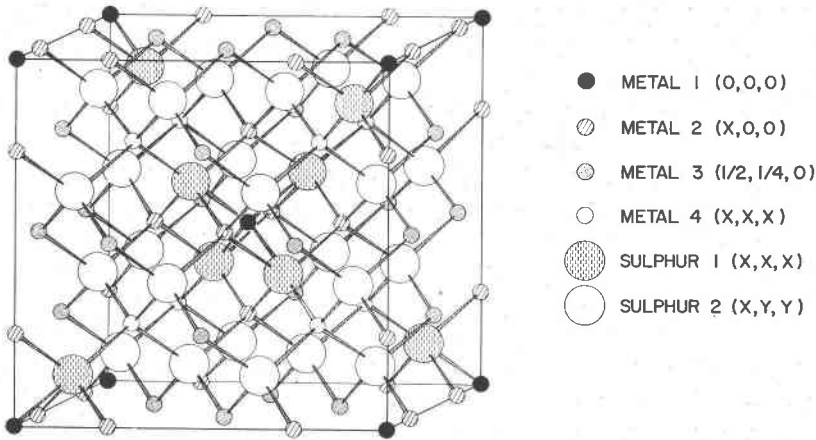- ▨ SULPHUR 1 (X,X,X)
- ◯ SULPHUR 2 (X,Y,Y)

FIG. 1. Unit cell model showing the crystal structure of talnakhite determined in this analysis. It is essentially equivalent to the structure of the synthetic β-phase (Hiller and Probsthain, 1956.)

origin translation (1/4, 1/4, 1/4). Structure factors were calculated assuming this model, with 32 S atoms at the $I\bar{4}3m$ sites $8c(1/8, 1/8, 1/8)$ and $24g(1/8, 3/8, 3/8)$; and 32 (Cu, Fe) atoms at the sites $12e(1/4, 0, 0)$, $12d(1/4, 1/2, 0)$, and $8c(1/4, 1/4, 1/4)$. The overall isotropic tempera-ture factor was 1.1Å^2. This and all subsequent calculations were per-formed on a Univac 1180 computer using the programs in the XRAY crystallographic system.[1] The Cu, Fe, and S atomic scattering factors were those of Cromer and Waber (1965), calculated using relativistic Dirac–Slater wave functions. The scattering factor for the (Cu, Fe) atoms was approximated as the average $[f(\text{Cu}) + f(\text{Fe})]/2$. The agree-ment between observed and calculated structure factors resulted in a R-value of 0.31. A difference $(|F_o| - |F_c|)$ synthesis was calculated to determine the difference between the sphalerite–like model and the true structure. The only major electron density residual in the synthesis was at the cell origin. This suggested that the site $2a(0, 0, 0)$ was occupied by the two additional metals which had been excluded from the sphalerite–like model. Agreement between the structure factors, calculated with the two (Cu, Fe) atoms at the $2a$ sites, and the observed data improved considerably and resulted in an R-value of 0.22. This showed that the structure of talnakhite was essentially consistent with the model proposed for the β–phase by Hiller and Probsthain (1956). The structure is shown diagrammatically in Figure 1.

[1] Stewart, J. M., F. A. Kundell, and J. C. Baldwin (1970) The XRAY system of crystallographic programs. *Computer Science Centre Report, U. of Maryland.*

With the inclusion of the additional two metal atoms [the (Cu, Fe) atoms will subsequently be referred to as metal or M atoms], the most significant features in the difference maps could be attributed either to shifts of certain metal and sulphur atoms from the ideal sphalerite–like sites or to changes in individual atomic temperature factors. These features were well–defined so that manual adjustment of the coordinates and isotropic thermal parameters, in a series of structure factor–difference synthesis calculations, quickly improved the agreement R–value for the observed reflections to 0.071. At this stage the only significant features in the difference map were *negative* residual shells, roughly spherical in shape, surrounding each of the metal sites. This indicated that the calculated radial distribution of electron density was excessively high beyond about 0.2Å from the atom center and, in turn, that the calculated scattering was too large at low Bragg angles. These features appeared to result either from using an atomic scattering curve which was excessively high at low $\sin \theta/\lambda$ values, or from a combination of too high a site occupancy and too high a temperature factor.

The latter of these two possibilities was less likely however, because the average temperature factor of the metals was not high $(\sim1.3\text{Å})^2$ and the site enclosed in the most pronounced negative shell had the lowest temperature factor $(0.80\text{Å})^2$. In addition, the postulated model of 34 M atoms and 32 S atoms agreed closely with the actual composition and, apart from some residual about the metal sites, there were no other features in the difference map to suggest that the metals were situated in other sites. On the other hand, a neutral scattering curve had been used for the metal atoms up to this point whereas Mössbauer and magnetic susceptibility measurements (Cabri and Goodman, 1970; Townsend *et al.*, 1971) indicate talnakhite is essentially antiferromagnetic similar to chalcopyrite (Donnay *et al.*, 1958). This implies that, like chalcopyrite, the metals are probably in the form of Cu^+ and Fe^{3+} ions. A scattering curve was therefore prepared from the average of the Cu^+ and Fe^{3+} curves of Cromer and Waber (1965). Structure factors were calculated using the average ionized curve for the metal atoms and the S^{2-} curve of Tomiie and Stam (1958), and this improved the agreement R–value to 0.059.

Although this lent support to the concept of positivily ionized metal atoms, no attempt had been made up to this point to establish the ordering of the copper or iron atoms at specific metal sites. The symmetry of the space group $I\bar{4}3m$ does not permit the complete ordering of Cu and Fe atoms in a sphalerite–like structure while still maintaining a stoichiometry of $Cu_{18}Fe_{16}S_{32}$. This inherent requirement for disorder

of the metals was also recognised by Hiller and Probsthain in deriving the structure of β–phase with the composition $Cu_{17.6}Fe_{17.6}S_{32}$. This, of course, does not exclude the possibility that *some* of the metal sites are occupied by one metal type. In fact, the concept of both order and disorder at the metal sites of talnakhite must be favoured over complete metal disorder for two reasons. First, the formation of the large cubic cell (10.6Å), over the smaller disordered cubic cell (5.3Å) proposed for high-temperature chalcopyrite (Donnay and Kullerud, 1958; Yund and Kullerud, 1966), implies a longer-range ordering of the metals. Second, the information available to date on the magnetic structure of talnakhite, suggests an ordering of metals not dissimilar to that of chalcopyrite.

A difference systhesis calculated with the metals as averaged (Cu^+, Fe^{3+}) atoms was examined for features that might indicate specific ordering of these atoms. Two of the sites did appear to have residual features in their environment which were different from the rest. The $2a$ site was still enclosed in a roughly spherical shell of negative residual density which indicated that the atom at this site may require a higher positive ionization than that provided by the scattering curve $[f(Cu^+) + f(Fe^{3+})]/2$. The other site, 8c, was enclosed in a similar but *positive* shell of residual, suggesting that this atom should have less positive ionization. Structure factors calculated as before, but with an Fe^{+3} atom at site $2a$ and a Cu^+ atom at site 8c, decreased the R–value to 0.054. This improvement in agreement could not in itself be considered very significant but certainly this configuration now had to be considered on equal footing with the complete disorder structure for the remainder of the refinement. The difference maps now contained no pronounced features that could be attributed to coordinate or isotropic thermal parameter shifts. However, there were asymmetric residual features about some sites that indicated the possibility of thermal anisotropy. There was also a positive peak of about $5e\text{Å}^{-3}$ at (1/2, 0, 0) indicating that the metal atoms partially occupy the site 6b. This is similar to the β–phase structure. The difference map gave no further evidence of metal ordering at specific sites. In addition, a interatomic distance calculation showed no significant differences in the various metal–sulphur distances that could be related directly to specific Fe–S and Cu–S bonds as found in chalcopyrite (Pauling and Brockway, 1932).

All subsequent refinement of coordinate and thermal parameters was performed by structure factor least squares, using the program CRYLSQ written by F. A. Kundell for the XRAY system. The two atomic arrangements (models A and B) which were considered are described in Table 1. Each model was refined with 3 cycles of isotropic

S. R. HALL AND E. J. GABE

TABLE 1

Structure Models A and B

Each model was refined using 3 rounds of isotropic full-matrix
SFLS (50 parameters, 13 variables) and 3 rounds of anisotropic full-matrix
SFLS (85 parameters, 20 variables).

| Atom | Site | Scattering Factors | |
		Model A	Model B
M(1)	2a	$[\underline{f}(Cu^+) + \underline{f}(Fe^{3+})]/2$	$\underline{f}(Fe^{3+})$
M(2)	12e	$[\underline{f}(Cu^+) + \underline{f}(Fe^{3+})]/2$	$[\underline{f}(Cu^+) + \underline{f}(Fe^{3+})]/2$
M(3)	12d	$[\underline{f}(Cu^+) + \underline{f}(Fe^{3+})]/2$	$[\underline{f}(Cu^+) + \underline{f}(Fe^{3+})]/2$
M(4)	8c	$[\underline{f}(Cu^+) + \underline{f}(Fe^{3+})]/2$	$\underline{f}(Cu^+)$
M(5)*	6b	$[\underline{f}(Cu^+) + \underline{f}(Fe^{3+})]/2$	$[\underline{f}(Cu^+) + \underline{f}(Fe^{3+})]/2$
S(1)	8c	$\underline{f}(S^{2-})$	$\underline{f}(S^{2-})$
S(2)	24g	$\underline{f}(S^{2-})$	$\underline{f}(S^{2-})$

*The occupancy of Metal 5 was refined during the 3 rounds of isotropic least
squares with a fixed isotropic temperature factor of $1.0 Å^2$.

and 3 cycles of anisotropic full–matrix least squares using unit weights.
The isotropic thermal parameter of metal 5 at site 6b was held con-
stant at $1.0 Å^2$ but its occupancy was refined during the initial three
cycles. With the inclusion of a fractional metal at this site there ap-
peared no further evidence of atoms at the unoccupied interstitial sites.

The refined parameters for models A and B are shown in Table 2
and the structure factor magnitudes and phases are listed in Table
3[1] Anomalous dispersion corrections $\Delta f'$ and $\Delta f''$ were not included in

TABLE 2

Final Atomic Parameters and Standard Deviations (in parentheses)

The anisotropic temperature factors are expressed in the form $T=\exp[-2\pi(U_{11}a^{*2}h^2 + 2U_{12}a^*b^*hk + ...)]$. The
isotropic temperature factors (B in $Å^2$) were obtained from the initial rounds of isotropic SFLS refinement. The site
occupancies were not refined except in the case of metal M(5).

Atom	Site	Model	x/a	y/b	z/c	$U_{11} \times 10^2$	$U_{22} \times 10^2$	$U_{33} \times 10^2$	$U_{12} \times 10^2$	$U_{13} \times 10^2$	$U_{23} \times 10^2$	Occup-ancy	B
M(1)	2a	A	0	0	0	1.08(17)	1.08(17)	1.08(17)	0	0	0	1.00	0.91(14)
		B	0	0	0	0.83(17)	0.83(17)	0.83(17)	0	0	0		0.77(15)
M(2)	12e	A	.2570(4)	0	0	1.39(16)	1.76(9)	1.76(9)	0	0	-.01(43)	1.00	1.30(5)
		B	.2571(4)	0	0	1.32(15)	1.66(9)	1.66(9)	0	0	.16(34)		1.23(5)
M(3)	12d	A	1/2	1/4	0	1.70(16)	1.55(9)	1.55(9)	0	0	.00	1.00	1.27(5)
		B	1/2	1/4	0	1.58(15)	1.47(8)	1.47(8)	0	0	0		1.18(5)
M(4)	8c	A	.2522(9)	.2522(9)	.2522(9)	1.71(8)	1.71(8)	1.71(8)	.02(11)	.02(11)	.02(11)	1.00	1.33(6)
		B	.2528(6)	.2528(6)	.2528(6)	2.04(8)	2.04(8)	2.04(8)	-.02(11)	-.02(11)	-.02(11)		1.58(6)
M(5)	6b	A	1/2	0	0							0.04(2)	1.00
		B	1/2	0	0								1.00
S(1)	8c	A	.1250(9)	.1250(9)	.1250(9)	1.80(35)	1.80(35)	1.80(35)	-.29(20)	-.29(20)	-.29(29)	1.00	1.55(20)
		B	.1245(9)	.1245(9)	.1245(9)	1.54(35)	1.54(35)	1.54(35)	-.18(26)	-.18(26)	-.18(26)		1.36(22)
S(2)	24g	A	.1207(7)	.3740(5)	.3740(5)	1.32(36)	1.20(20)	1.20(20)	-.04(14)	-.04(14)	.03(27)	1.00	0.94(6)
		B	.1209(7)	.3737(6)	.3737(6)	1.23(37)	1.29(21)	1.29(21)	-.03(16)	-.03(16)	-.09(28)		0.95(7)

[1] To obtain a copy of this material, order NAPS Document No. 01717 from
National Auxiliary Publications Service of the A.S.I.S., c/o CCM Information
Corporation, 866 Third Avenue, New York, N. Y. 10022; remitting $2.00 for
microfiche or $5.00 for photocopies, in advance, payable to CCMIC-NAPS.

the least squares process but were applied to each model in a structure factor calculation on completion of the refinement. The corrections used were $\Delta f'_{Cu} = 0.36$, $\Delta f'_{Fe} = 0.37$, $\Delta f'_{S} = 0.13$, $\Delta f''_{Cu} = 1.36$, $\Delta f''_{Fe} = 0.92$, and $\Delta f''_{S} = 0.16$ (Cromer, 1965). The final R–values were 0.053 for Model A with no anomalous dispersion corrections, 0.060 for model A with $\Delta f'$ and $\Delta f''$ corrections, and 0.066 for the inverse of model A with $\Delta f'$ and $\Delta f''$ corrections. The R–values for the equivalent calculation on model B were 0.045, 0.051, and 0.060. Correction for secondary extinction was not applied to the F_o–data both because of the high mosaicity of the talnakhite crystals and the lack of consistent evidence for this effect in the I_o/I_c ratios.

DESCRIPTION OF THE STRUCTURE

The atomic coordinates of talnakhite, listed in Table 2, do not vary significantly for the two atomic arrangements. These values provide, to reasonably accuracy, the displacements of the atoms from the idealized sphalerite sites. On the other hand the thermal motion and occupancy parameters, also listed in Table 2, are of questionable reliability. This is not only to the interaction of these two types of parameters in an X-ray structure refinement but also to the lack of conclusive information about the ordering and ionization of the Cu and Fe atoms. Therefore comparison of the two refinement models can only be, at best, qualitative, and no attempt has been made to accurately balance the total charge of the anions and cations. Also, in the absence of conclusive X-ray evidence, it should be stressed that models refined in this analysis represent only two of a number of possible atomic arrangements and that conclusive identification of the true metal ordering and ionization must await additional information from other techniques.

The structure of talnakhite is similar, both in cell and atomic arrangement, to that of binnite $Cu_{12}As_4S_{13}$ (Wuensch *et al.*, 1965) and of tetrahedrite $Cu_{12}Sb_4S_{13}$ (Wuensch, 1964). The similarity of these minerals in diffraction aspect had been reported previously (Cabri, 1967). This study shows, however, that the talnakhite structure differs in two important respects from the structures of binnite and tetrahedrite. First, metal atoms are located at site $2a$ in talnakhite while there are sulphurs in binnite and tetrahedrite. Second, the eight sulphur atoms at site $8c$ in talnakhite are absent in the other two structures. These departures give rise to a significantly different distortion of the atoms from the sphalerite–like sites and make further comparison of these structures unwarranted.

The interatomic distances and angles, calculated using the coordi-

nates from models A and B in Table 2, do not differ significantly. These values are listed for model A in Table 4 and are shown diagrammatically in Figure 2. Three atoms show substantial shifts away from the idealized sphalerite sites, with $M(2)$ having the largest displacement of 0.075Å. This consistent with the inclusion of the atom $M(1)$ at site $2a$, which is intersitial to the sphalerite structure. Despite this shift, the $M(1)–M(2)$ distance of 2.72Å is significantly shorter than a close Fe–Fe contact of 2.82Å in cubanite $CuFe_2S_3$ (Fleet, 1971) but longer than a comparable (Fe,Ni)–(Fe,Ni) distance of 2.52Å in pentlandite (Fe, Ni)$_9$S$_8$ (Pearson and Buerger, 1959). Comparison of the metal–metal distances between these structures is difficult, however, due to the substantially different environments of the metal atoms. In the structure of cubanite, the FeS$_4$ tetrahedra share one common edge but, in pentlandite, the (Fe, Ni)S$_4$ tetrahedra share three edges. In talnakhite, each $M(2)$S$_4$ tetrahedron shares an edge with one $M(1)$S$_4$ tetrahedron, and as a consequence, the latter shares all *six* of its edges. This results in a close second-neighbour octahedral coordination of $M(2)$ atoms about the $M(1)$ atom. Therefore the struc-

TABLE 4

Interatomic Distances and Angles

Calculated from coordinates in Table 2, model A.   Standard deviations are in parentheses.

Distances (in Ångstroms)			Angles (in degrees)		
S(1) – M(1)	2.293	(13)	M(1) – S(1) – M(2)	72.0	(3)
S(1) – M(2)	2.337	(13)	M(1) – S(1) – M(4)	180.0	(3)
S(1) – M(4)	2.334	(13)	M(2) – S(1) – M(2)	110.9	(3)
			M(2) – S(1) – M(4)	108.0	(3)
S(2) – M(2)	2.289	(13)			
S(2) – M(3)	2.268	(13)	M(2) – S(2) – M(3)	108.3	(3)
S(2) – M(4)	2.295	(13)	M(2) – S(2) – M(4)	108.2	(3)
S(2) – M(5)	2.280	(13)	M(2) – S(2) – M(5)	68.6	(3)
			M(3) – S(2) – M(3)	111.3	(3)
S(1) – S(1)	3.744	(19)	M(3) – S(2) – M(4)	110.3	(3)
S(1) – S(2)	3.731	(19)	M(3) – S(2) – M(5)	71.2	(3)
S(1) – S(2)*	3.785	(19)	M(4) – S(2) – M(5)	176.8	(3)
S(2) – S(2)	3.794	(19)	S(1) – M(1) – S(1)	109.5	(3)
S(2) – S(2)*	3.775	(19)			
S(2) – S(2)*	3.697	(19)	S(1) – M(2) – S(1)	106.5	(3)
S(2) – S(2)*	3.706	(19)	S(1) – M(2) – S(2)	109.8	(3)
			S(2) – M(2) – S(2)	111.1	(3)
M(1) – M(2)	2.722	(18)			
			S(2) – M(3) – S(2)	109.2	(3)
M(2) – M(2)	3.850	(19)	S(2) – M(3) – S(2)*	109.6	(3)
M(2) – M(3)	3.693	(18)			
M(2) – M(4)	3.714	(19)	S(1) – M(4) – S(2)	107.4	(3)
M(2) – M(4)*	3.778	(19)	S(2) – M(4) – S(2)	111.5	(3)
M(2) – M(5)	2.574	(18)			
			S(2) – M(5) – S(2)	108.3	(3)
M(3) – M(3)	3.745	(19)	S(2) – M(5) – S(2)*	111.8	(3)
M(3) – M(4)	3.745	(19)			
M(3) – M(5)	2.648	(18)			

*The preceding interatomic distance on angle in the list is between atoms at different but equivalent sites.
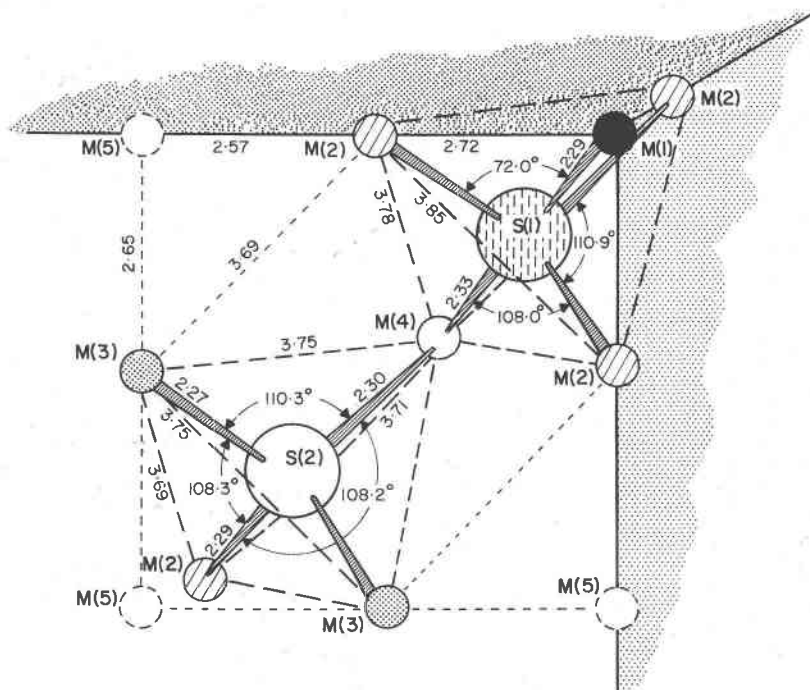
FIG. 2. A partial structure model of talnakhite showing the metal coordination about the two independent sulphur atoms with selected interatomic distances (in Ångstroms) and angles (in degrees) calculated for model *A*.

ture of talnakhite, unlike that of either cubanite or pentlandite, contains both asymmetric (about the $M(2)$ atom) and symmetric (about the $M(1)$ atom) second-neighbour metal coordination. The nature of the electronic interaction between these atoms, particularly in the absence of real evidence to their identity, is not understood.

The fivefold coordination of the metals about the $S(1)$ atom can be described as a distorted trigonal bi–pyramid (see Figure 2). Four of these atoms, three $M(2)$ and one $M(4)$, form angles close to tetrahedral and the fifth, $M(1)$, forms a bond parallel to $S(1)-M(4)$ and a $M(1)-S(1)-M(2)$ angle of 72.0°. This compares with a similar Fe–S–Fe angle of 74.7° in cubanite (Fleet, 1971).

The other two major displacements of atoms from the sphalerite–like sites can also be attributed to the inclusion of $M(1)$ at the site $2a$. The $S(2)$ atoms, which share the edge of the $M(2)$ tetrahedra, are 0.045Å from the idealized site. The $S(2)$ atom has essentially shifted in a parallel direction to the displacement of $M(2)$, but slightly away. This results in a $S(2)-M(2)$ distance of 2.289Å close to the
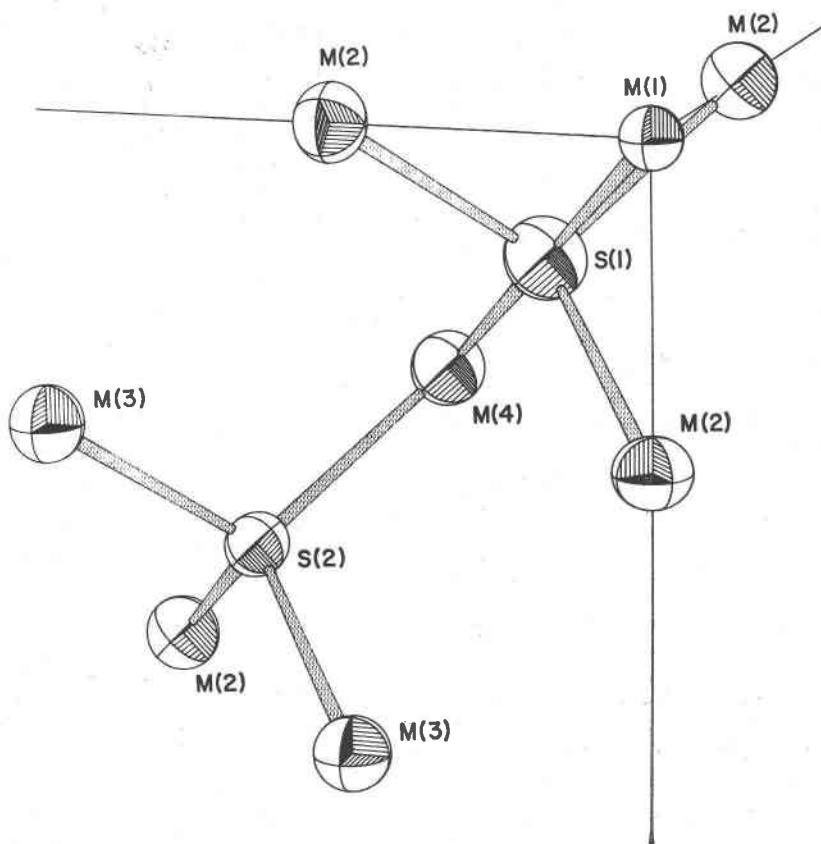
Fig. 3. A partial structural model of talnakhite showing the atomic thermal ellipsoids of model A plotted at the 90 percent probability level.

"ideal" distance of 2.293Å. As S(2) shifts towards the tetrahedron edge bounded by M(3) this reduced the S(2)–M(3) distance to 2.268Å.

The only other significant atomic change from the idealized structure is the 0.037Å shift of M(4), along the 3–fold rotor axis of the cell, towards the tetrahedron face bounded by three S(2) atoms. The shifts of the S(2) atoms in the plane of this face but directly away from the center, appears sufficient to move the equilibrium centre of the tetrahedron and, consequently, the M(4) atom towards this face.

The anisotropic U_{ij} thermal paramenters are listed in Table 2 and displayed diagrammically in Figure 3 as thermal displacement

ellipsoids. The ellipsoids were drawn using the program ORTEP (Johnson, 1965). These show that the thermal motion of both metals and sulphur atoms is essentially isotropic. Both the $M(3)$ and $S(2)$ atoms have thermal ellipsoids flattened in the direction of their displacement from the idealized sphalerite sites but this cannot be considered significant with respect to the standard deviations. Similarly, the elongation of the $M(3)$ thermal ellipsoids is probably not real, as suggested by the reversal of anisotropic components in the refinement of models A and B. It is most probable, particularly as the ratio of reflection data to atomic variables in the least squares refinement process is not high (see Table1), that some anisotropic parameters are compensating for errors in the data, or for asymmetric electron residual in the structure not necessarily due to thermal motion effects. Variations in isotropic temperature factor are probably not reliable for similar reasons. This is especially true because the effects of site occupancy and its interaction with ionized scattering curves constitute a symmetric effect that is difficult to distinguish from variation in isotropic thermal motion. Because of this, no attempt was made to refine site occupancy, except in the case of $M(5)$ where the value is low (4 percent). Similarly, the low thermal parameters for $M(1)$ do not appear significant, though they would be consistent with the constraints placed on this atom by its closely packed environment.

REFERENCES

BUD'KO, I. A., AND E. A. KULAGOV (1963) Natural cubic chalcopyrite. *Dokl. Akad. Nauk. SSSR* 152, 408–410 [English transl. *Dokl. Acad. Sci. USSSR, Earth Sci. Sect.* 152, 135–147 (1965).]

BUSING, W. R. (1970) Least squares refinement of lattice and orientation parameters for use in automatic diffractometry. *In* F. R. Ahmed, (ed.) *Crystallographic Computing.* Munksgaard, Copenhagen, 319–330.

CABRI, L. J. (1967). A new copper iron sulphide. *Econ. Geol.* 62, 910–925.

———, AND R. H. GOODMAN (1970) Mössbauer spectra of copper-iron sulphides. *Geokhimiya,* 636–639 [English transl. *Geochem. Internat.* 7, 453–455 (1970).]

————, AND D. C. HARRIS (1971) New compositionl data for talnakhite, $Cu_{18}(Fe,Ni)_{18}S_{32}$. *Econ. Geol.* 66, 673–675.

CROMER, D. T. (1965) Anomalous dispersion corrections computed from self-consistent field relativistic Dirac-Slater wave functions. *Acta Crystallogr.* 18, 17–23.

————, AND J. T. WABER (1965) Scattering factors computed from Dirac-Slater wave functions. *Acta Crystallogr.* 18, 104–109.

DONNAY, G. L. M. CORLISS, J. D. H. DONNAY, N. ELLIOT, AND J. M. HASTINGS (1958) Symmetry of magnetic structures:magnetic structure of chalcopyrite. *Phys. Rev.* 112, 1917–1923.

————, AND G. KULLERUD (1958) High temperature chalcopyrite. *Carnegie Inst. Wash. Year Book* 57, 246.

FLEET, M. E. (1971) Refinement of the crystal structure of cubanite and polymorphism of $CuFe_2S_3$. *Z. Kristallogr.* 132, 276–287.

GABE, E. J., AND T. O'BYRNE (1970) An absorption correction program for the PDP-8. *Amer. Crystallogr. Ass. Summer Meet., Ottawa, Abstr. Pap.* A4.

GENKIN, A. D., A. A. FILIMONOVA, T. N. SHADLUN, S. V. SOBELEVA, AND N. V. TRONEVA (1966) On cubic cubanite and cubic chalcopyrite. *Geol. Rud. Mestor, Zhd.* 8, 41–54 [English transl. *Geochem. Internat.* 766–781 (1965).]

HILLER, J. E., AND K. PROBSTHAIN (1956) Thermische und röntgenographische untersuchungen am Kupferkies. *Z. Kristallogr.* 108, 108–129.

JOHNSON, C. K. (1965) ORTEP Fortran thermal ellipsoid plot program for crystal structure illustrations. *U.S. Clearinghouse Fed. Sci. Tech. Info. Rep.* ORNL-3794.

PAULING, L., AND L. O. BROCKWAY (1932) The crystal structure of chalcopyrite. *Z. Kristallogr.* 82, 188–194.

PEARSON, A. D., AND M. J. BUERGER (1956) Confirmation of the crystal structure of pentlandite. *Amer. Mineral.* 41, 804–805.

TOMIIE, Y., AND C. H. STAM (1958) Calculation of atomic scattering factors using Slater wave functions:sodium to calcium. *Acta Crystallogr.* 11, 126–127.

TOWNSEND, M. G., J. L. HORWOOD, S. R. HALL, AND L. J. CABRI (1971) Mössbauer, magnetic susceptibility and crystallographic investigations of $Cu_4Fe_4S_8$, $Cu_{18}Fe_{16}S_{32}$ and $Cu_9Fe_9S_{16}$. *17th Conf. Magn. Magn. Mater. Abstr.*, paper 2H-13.

WUENSCH, B. J. (1964) The crystal structure of tetrahedrite, $Cu_{12}Sb_4S_{13}$. *Z. Kristallogr.* 119, 437–453.

————, J. TAKÉUCHI, AND W. NOWACKI (1965) Refinement of the crystal structure of binnite, $Cu_{12}As_4S_{13}$. *Z. Kristallogr.* 123, 1–20.

YUND, R. A., AND G. KULLERUD (1966) Thermal stability of assemblages in Cu-Fe-S system. *J. Petrology,* 7, 454–488.